FISEVIER

Contents lists available at ScienceDirect

# Palaeogeography, Palaeoclimatology, Palaeoecology

journal homepage: www.elsevier.com/locate/palaeo



# Late Miocene drying of central Australia

Xuegang Mao<sup>a,b</sup>, Gregory Retallack<sup>b,\*</sup>

- <sup>a</sup> Institute of Geography, Fujian Normal University, Fuzhou 350007. China
- <sup>b</sup> Department of Earth Science, University of Oregon, Eugene, OR 97403-1272, USA



Keywords: Laterite Caliche Paleosol Paleoclimate Mulga Rainforest

#### ABSTRACT

A back to the future approach to climate change refines Neogene records of paleoclimatic cooling and drying as future climate states for a warming world. Near Alcoota station in central Australia is a late Miocene fossil mammal site for Alcoota (10 Ma) and Ongeva (8 Ma) local faunas. The Alcoota fauna includes the largest known land bird (Dromornis stirtoni) and early diprotodontid (Kolopsis torus), but the geologically younger Ongeva fauna has a larger diprotodontid (Zygomaturus gilli). These faunas are evolutionary predecessors of Australian Pleistocene megafauna. Calcareous paleosols recorded a marked turn toward aridity compared with underlying thick lateritic duricrusts which lack fossils. Laterites of likely middle Miocene age are evidence of wet (> 1100 mm mean annual precipitation) tropical (> 17 °C mean annual temperature) paleoclimates, but these were deeply eroded and redeposited by the time of the late Miocene mammals. A succession of 19 paleosols of 5 pedotypes were recognized in the 19 m thick section, with shallow calcareous nodule (Bk) horizons as evidence of mean annual precipitation ranges from 100 to 400 mm, and mean annual range of precipitation of 50 mm, very similar to the modern climate of Alcoota (296 mm precipitation with 56 mm difference between wet and dry month). This was neither a rainforest nor monsoonal paleoclimate, and vegetation inferred from paleosols was open woodland and gallery woodland similar to that of today. Central Australia was not covered by monsoon rainforest during the late Miocene and its paleoclimatic history of Neogene desertification matches well that of other parts of the world.

## 1. Introduction

Neogene paleoclimate records may be guides to climate change expected with increased carbon dioxide in the atmosphere, because the future will reverse Neogene cooling and drying now known from a variety of detailed proxies (Breecker et al., 2010; Beerling and Royer, 2011). Thus climate and vegetation of the future can be predicted by reconstructing plants, animals and soils of the past formed at times of known atmospheric carbon dioxide concentration (Retallack et al., 2018a). Estimates of 612  $\pm$  24 ppm atmospheric carbon dioxide for the middle Miocene are of special interest because comparable with predicted carbon dioxide by the year 2100 with current emission scenarios (Retallack et al., 2016). One difficulty for predicting Australian future climate in this way is debate whether Miocene monsoon rain forest was widespread in central Australia (Archer et al., 1994; Travouillon et al., 2009) or limited to northern Australia (Megirian et al., 2004; Herold et al., 2011). Paleosols are useful to such a task because rainforest soils are thick lateritic or bauxitic duricrusts (Retallack, 2010), and aridity and monsoonal seasonality is reflected in patterns of pedogenic carbonate nodules (Retallack, 2005). This study

addresses paleoclimate and vegetation changes for two successive mammal assemblages in the late Miocene, Waite Formation near Alcoota, Northern Territory, Australia (Woodburne, 1967; Megirian et al., 1996; Murray and Vickers-Rich, 2004). These can be added to other records of Australian Neogene paleoclimate (Metzger and Retallack, 2010) for comparison with paleoclimatic records from paleosols in other parts of the world (Retallack, 1991a, 2007; Retallack et al., 2016, 2018a).

## 2. Geological background

The Alcoota local fauna from 150 km northeast of Alice Springs, central Australia (Fig. 1), has at least 25 species of vertebrates including the largest known land bird (*Dromornis stirtoni*) and early diprotodontid (*Kolopsis torus*: Megirian et al., 1996; Murray and Vickers-Rich, 2004) from a quarry at the base of our measured section (Figs. 2C, 3). A separate fauna of 6 vertebrate species including the large diprotodontid (*Zygomaturus gilli*: Megirian et al., 1996, 2010) were found at 9.5 m in our measured section (Fig. 3). The Alcoota local fauna is envisaged as a clayey waterhole which attracted animals during drought (Murray and

E-mail address: gregr@uoregon.edu (G. Retallack).

<sup>\*</sup> Corresponding author.

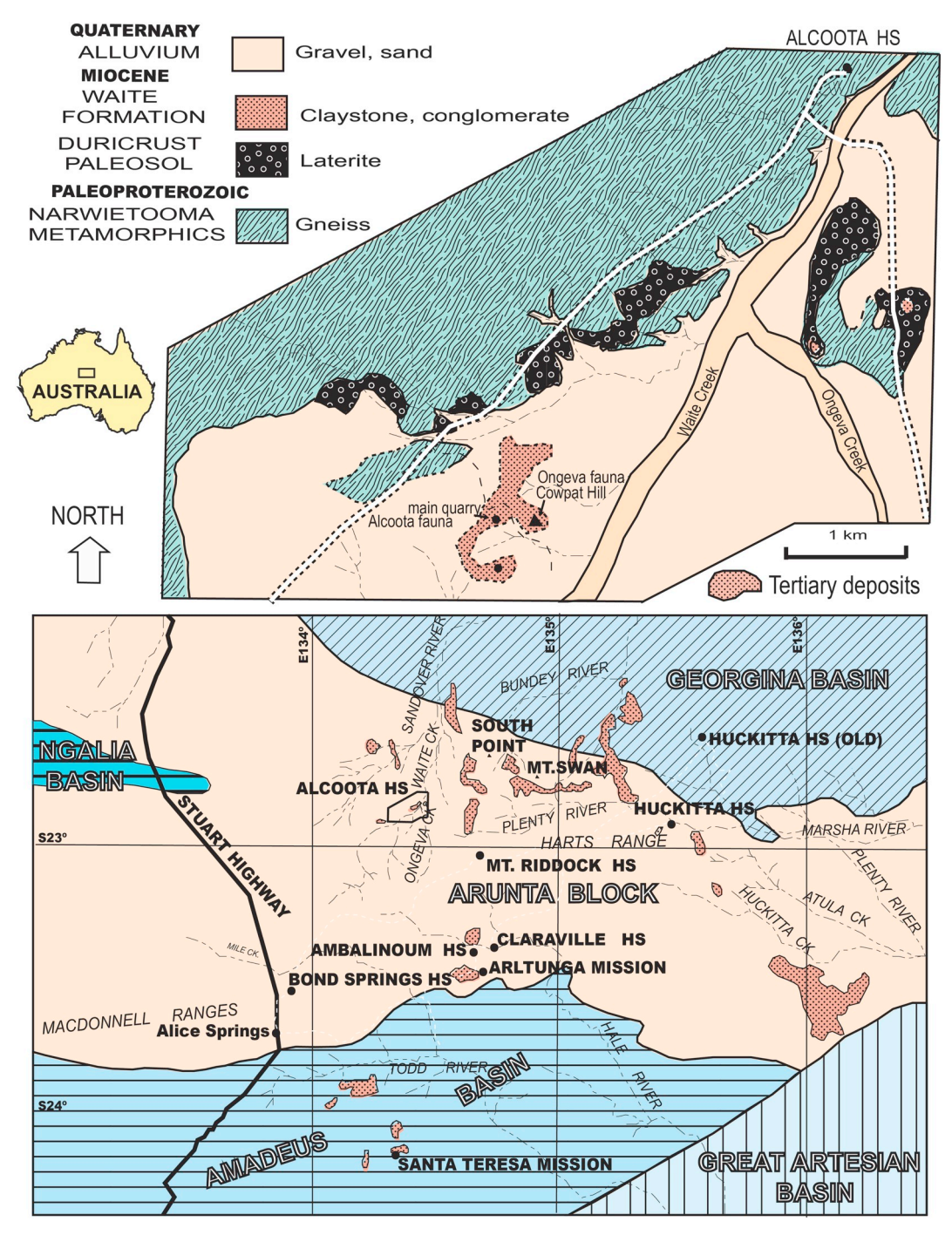


Fig. 1. Study area and geological map of Alcoota fossil beds, modified after Woodburne (1967).

Vickers-Rich, 2004), but the Ongeva local fauna is in sandy alluvial deposits (Megirian et al., 1996). The age of the Alcoota and Ongeva local faunas has been estimated between 5 and 12 Ma by biostratigraphic correlation of the Waitean Australian Land Mammal Age with comparable faunas in Victoria, where they are constrained by radiometric ages (Megirian et al., 2010). These lacustrine and fluvial deposits are the Waite Formation, which fills depressions in 10 m thick laterite above 14 m of saprolite (Woodburne, 1967) developed on gneiss of the Paleoproterozoic (> 1870 Ma), Narwietooma Metamorphics (Shaw and Warren, 1975; Rohde, 2005). The age of the laterite is constrained by formation on late Oligocene, Tug Member of the Hale Formation in the Hale Basin 40 km south of Alcoota (Senior et al., 1994). However, K-Ar and  $^{40}$ Ar/ $^{39}$ Ar dating of manganese oxides in the Groot Eylandt laterite

of Northern Territory shows that laterites mostly formed at 16, 26 and 29 Ma, with lesser peaks at 12, 17 and 42 Ma (Dammer et al., 1996). Middle Miocene laterite formation is most likely, because it was a global phenomenon, when laterites formed as far north as Portland, Oregon, and as far south as Sydney, Australia (Retallack, 2010).

## 3. Materials and methods

A geological section was measured from the main fossil quarry (Figs. 1–2) to the top of nearby Cowpat Hill (22.8617°S, 134.4214°E, 617 m elevation), 5.5 km southwest of Alcoota homestead, northeast of Alice Springs, central Australia. The present-day climate in this area has hot dry summer and cold winter. Paleosols were identified in the field

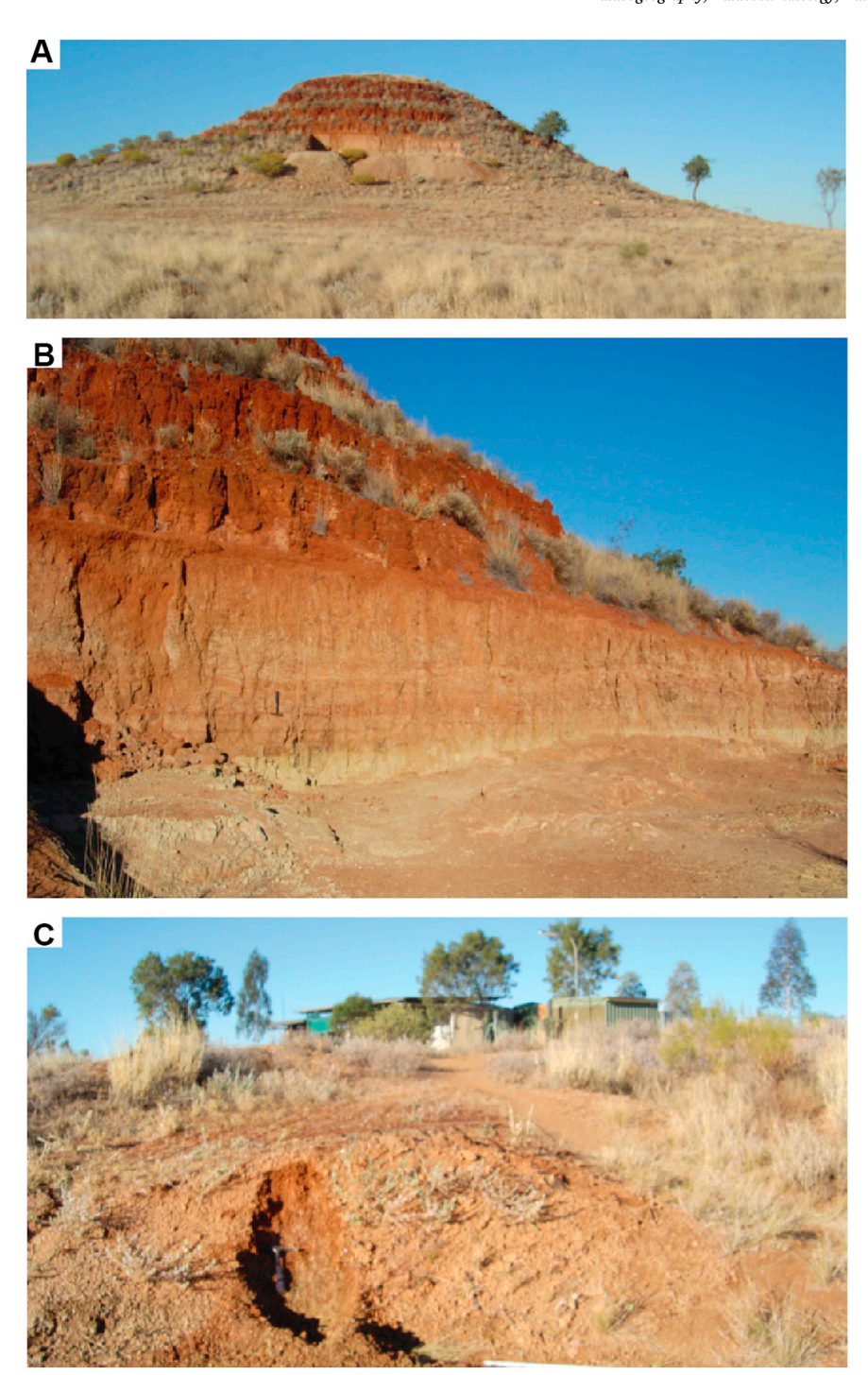


Fig. 2. Field images of the measured section: (A) overview of Cowpat Hill; (B) quarry for Ongeva local fauna in hill; (C) main quarry for Alcoota local fauna at base of section.

mainly based on root traces, soil horizons and soil structures (Fig. 3) and individual pedotypes were sampled for geochemical analysis and micromorphology in thin section (Fig. 4). Depth to calcareous nodules, thickness of paleosol with calcareous nodules, and nodule diameter were recorded because of their paleoenvironmental implications (Retallack, 2005). Paleosol development (weak, moderate, strong) was estimated from the degree to which sedimentary features were obscured by pedogenic features (Retallack, 2001). Calcareousness (weak, moderate, strong) was estimated by relative reaction with dilute (0.1 mol) HCl. Hue was recorded using a Munsell Color Chart. Petrographic thin sections were ground in kerosene to prevent clay

expansion (Tate and Retallack, 1995). Each thin section was point counted (500 points) for grain size and mineral content using a Swift automated stage and Hacker counting box. X-ray diffraction traces were made under Cu-Ni radiation using a Rigaku goniometer in the Department of Earth Sciences, University of Oregon, and custom Fortran code for migration to an Excel spreadsheet. Major elements were analyzed using X-ray fluorescence by ALS Chemex of Vancouver, BC, against CANMET standard SDMS2 (British Columbia granodioritic stream sand). Soil-forming chemical reactions evaluated by molar ratios of major elements (Retallack, 1991a). For example, molar ratio of Na<sub>2</sub>O/  $\rm K_2O$  is an indication of salinization, (CaO + MgO)/Al<sub>2</sub>O<sub>3</sub> of

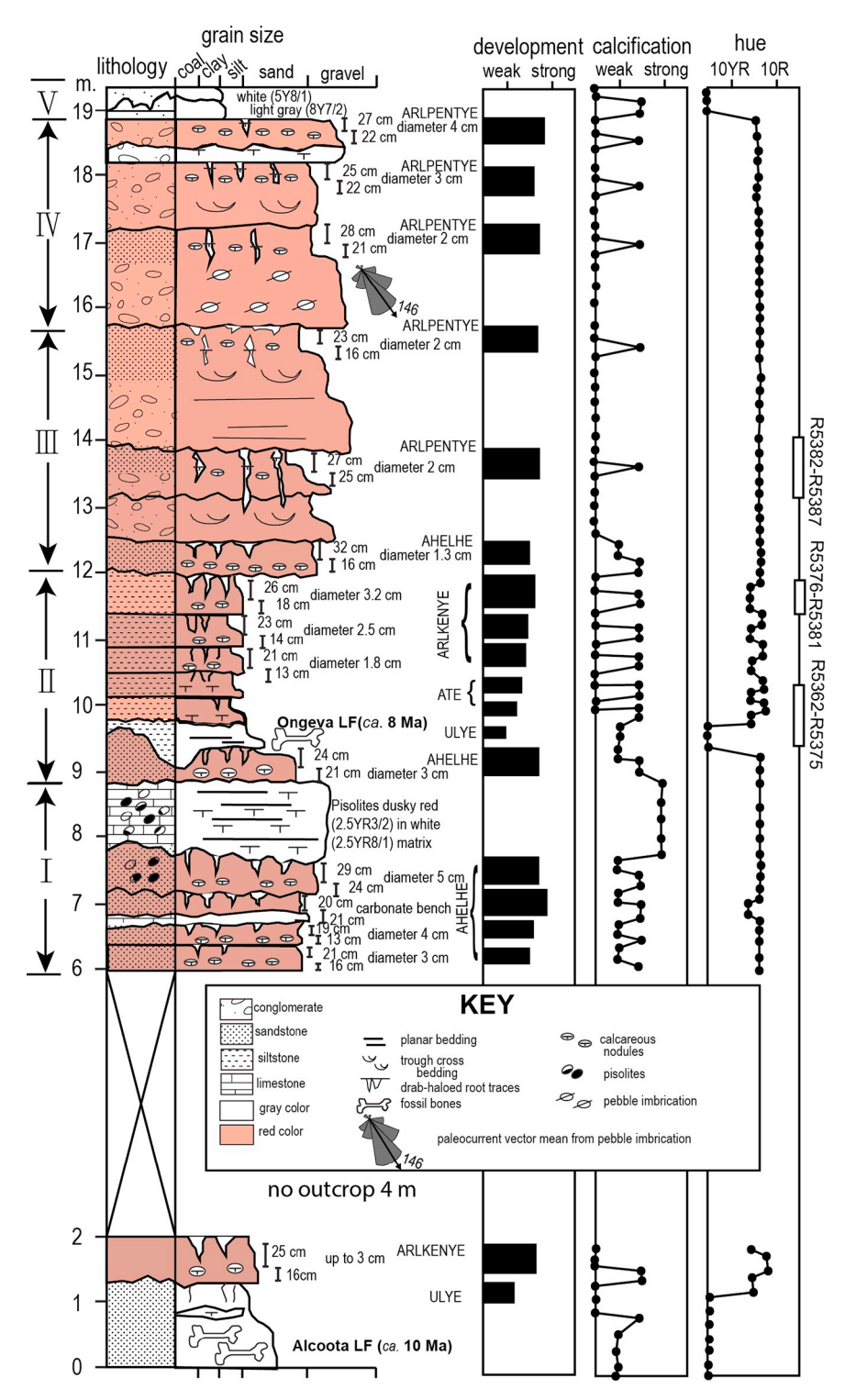


Fig. 3. Composite geological section of Cowpat Hill. Pedotype names are to the left of the development boxes (black rectangular boxes), based on the soil maturity (Retallack, 2001). Calcification as a guide to aridity is based on field reaction with dilute HCl (Retallack, 2001). Hue as a guide to waterlogging is based on Munsell Color Chart. Palaeocurrent direction from northwest to southeast at 16 m was obtained by calculating frequency of pebble dip angles in the imbrication structure.

calcification,  $Al_2O_3/SiO_2$  of clayeyness,  $Al_2O_3/(CaO + MgO + Na_2O + K_2O)$  of base loss, Ba/Sr of leaching, FeO/Fe<sub>2</sub>O<sub>3</sub> of gleization. Bulk density was measured by the clod method; comparing weight paraffincoated and uncoated of 10–20 g rock samples in both air and water (Retallack, 1997). All petrographic and chemical data are tabulated in Supplementary materials online.

Soil forming processes were modeled by computing mass transfer of elements (Brimhall et al., 1992) versus volume change (called strain  $\varepsilon_i$ ,

 $_w$  in mole fraction) and mass change (mass transfer  $\tau_{j,w}$  in mole fraction) compared with parent materials (defined as 0 strain and 0 mass transfer), the less weathered materials at the bottom of the observed profile. The relevant equations of strain  $\varepsilon_{i,w}$  and mass transfer  $\tau_{j,w}$  are below:

$$\varepsilon_{i,w} = \frac{\rho_p c_{i,p}}{\rho_w c_{i,w}} - 1 \tag{1}$$

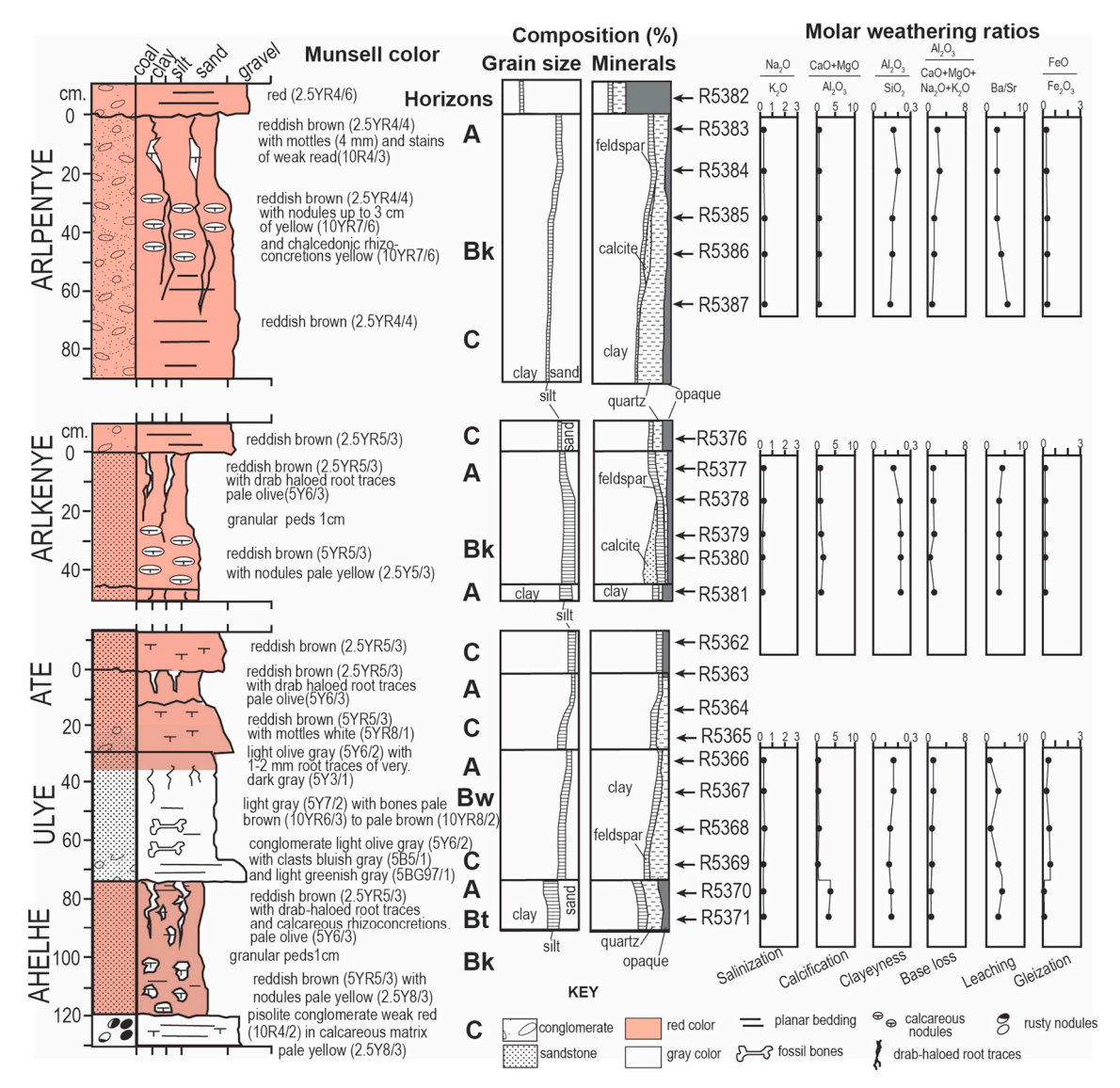


Fig. 4. Field observations, grain size and mineral content by point counting under petrographic thin section, and molecular weathering ratios of Ulye, Arlkenye, Arlpentye pedotypes in Cowpat section.

$$\tau_{j,w} = \frac{\rho_w c_{j,w}}{\rho_p c_{j,p}} (\varepsilon_{i,w} + 1) - 1 \tag{2}$$

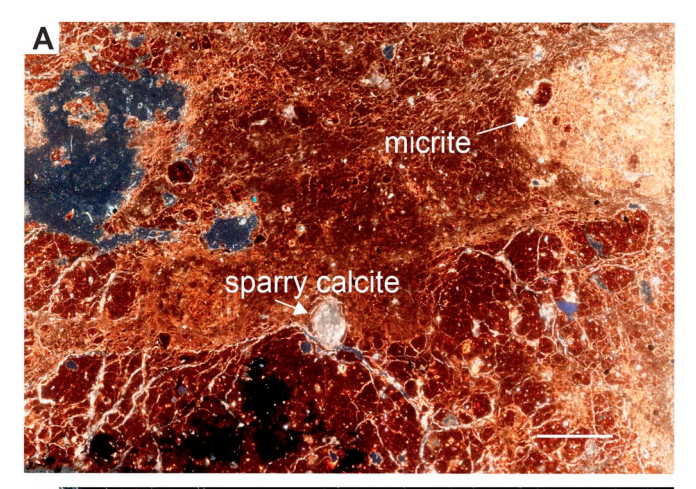
where  $\rho$  is bulk density in g/cm³, c is element concentration in wt%, i is immobile element (Ti used here), j is mobile element, p is parent material, w is weathered materials. Choice of parent material is critical to this kind of tau analysis, and our choice of lower parts of the profiles is supported by comparable  $Al_2O_3/SiO_2$  ratios and high clay content throughout the profiles (Fig. 4).

#### 4. Paleosol recognition

Root traces were conspicuous guides to paleosols near Alcoota, and consisted of drab-haloed root traces and also calcareous rhizoconcretions (Fig. 3). Most of the paleosols had calcareous Bk horizons of pedogenic carbonate nodules ranging from 1 to 5 cm diameter, but some had a solid bench of carbonate, and others were thin and weakly developed. There also were beds of lateritic pisolites, but in a calcareous matrix, indicating that they were redeposited as pedoliths, rather than in place lateritic profiles (Retallack, 2010). These pisolitic gravels, and other horizons of conglomerate with gneiss and vein-quartz pebbles are interbedded with massive red paleosols.

Paleosols recognized in the field were confirmed by point counting thin sections and a variety of molecular weathering ratios (Fig. 4). Sharp changes of grain size and mineral composition were found between sediment and paleosol in the profiles, but transitional changes within paleosols, consistent with field observations. Vertical distributions of calcite correspond well with Bk horizons, confirming calcification as the main soil-forming process (Retallack, 2001). There are subtle changes in clay content, mainly greatest toward the surface, that reveal little differentiation of clayey subsurface (argillic) horizons. There is no chemical indication of soda enrichment (salinization), which sometimes accompanies calcification (Retallack et al., 2018b). Alumina/silica, alumina/bases, and barium/strontium ratios are all higher than expected for calcareous desert soils (Retallack et al., 2003; Retallack, 2012b). These anomalies are evidence of parent material derived from pisolitic laterite and deeply weathered saprolite like that underlying the Waite Formation (Woodburne, 1967; Megirian et al., 1996).

Thin sections also reveal little remnant sedimentary structure and porphyroskelic, mosepic to isotic soil fabrics (Supplementary Table S1). Some thin sections show carbonate cementation with spar-filled root traces and replacive micritic nodules (Fig. 5A). Other thin sections show sand-size grains floating in clayey matrix, and sometimes grain



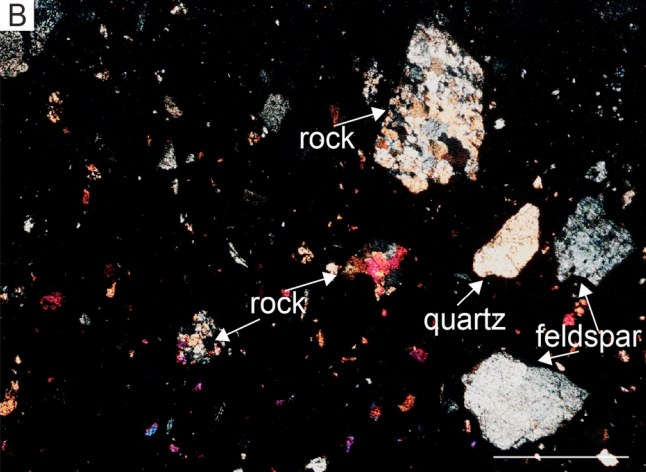


**Fig. 5.** Petrographic thin sections of paleosols (A) and parent materials (B). (A) is from Bk horizon of Arlkenye pedotype (R5380), characteristic of pedogenic calcite (micrite and sparry calcite) and abundant and stress-oriented clay (red). (B) is from C horizon of Ate pedotype (R5365), characteristic of eroded rock fragments, sand-sized quartz and feldspars. Both are under cross nicols. Both bars represent 2 mm. (For interpretation of the references to color in this figure legend, the reader is referred to the web version of this article.)

fragmentation and dissolution of labile grains (Fig. 5B).

A more sophisticated demonstration of soil formation is tau analysis. Soil development can be distinguished from sediment accumulation by tau analysis of mass and volume change, because both are negative in soil but positive in sediment. Only three pedotypes had parent material samples adequate to this analysis. As seen in Fig. 6, all three paleosols are largely within the collapse-and-loss quadrant, though some elements (e.g. Mg, Na, Al, Fe<sup>3+</sup>) have positive mass transfer, suggesting pedogenic enrichment.

## 5. Paleosol diagenesis

Soil formation is a form of early diagenesis, or alteration after deposition, but additional alteration after burial requires assessment for interpretation of paleosols. Three common burial alterations are evident in paleosols of Alcoota: burial decomposition of organic matter in A horizons, burial gleization of remnant organic matter in roots, and dehydration of ferric hydroxides to hematite (Retallack, 1991b). This would have changed colors to lighter gray in surface horizons and red rather than brown in matrix, and also left prominent green root haloes that were not in the original soil. The illite peaks at 8.9 20 on the X-ray diffractogram (Fig. 7) are broad and low, like pedogenic rather than metamorphic clays. Metamorphic clays have a Weaver index (height

above background at  $10\ \text{Å/height}$  above background at  $10.5\ \text{Å}) > 2.3$ , but Weaver indices for our samples are 1.5, 2.0, and 2.1 respectively for specimens R5366, R5377, and R5383. Metamorphic clays have a Kübler index (20 width at half height of  $10\ \text{Å}$  peak) < 0.42, but our samples have Kübler indices 0.7, 1.1 and 0.8 respectively. Nor is there any evident potash enrichment (Fig. 6), often observed with burial illitization (Novoselov and de Souza Filho, 2015). Burial compaction can be corrected using standard curves (Sheldon and Retallack, 2001), but compaction effects for only  $19\ \text{m}$  of burial are insignificant, especially when offset by pervasive cementation with hematite and calcite.

#### 6. Paleosol classification and interpretation

Many successive paleosols were identical in profile form so that the 19 successive profiles were classified into 5 distinct pedotypes named using Arrernte language spoken in northern and central Australia (Green, 1994; Henderson and Dobson, 1994). Table 1 summarizes diagnostic features and classification of the five pedotypes in classifications of US soil taxonomy (Soil Survey Staff, 2014), the old Australian classification (Stace et al., 1968), and the FAO soil map of the world (FAO, 1974). The paleosols are identified as Calcids rather than Argids (of Soil Survey Staff, 2014), because the clay is kaolinitic and inherited as sedimentary parent material, rather than pedogenic. The classification is non-genetic, but can be used to identify comparable modern soilscapes. The ancient soilscape for both the Alcoota and Ongeva local fauna levels was dominated by Calcic Xerosols (Xk) with minor Eutric Fluvisols (Je) and Haplic Phaeozems (Hh). The most similar modern soilscape in central Australia is map unit Xk46-2ab with associated Xh and Hh around Lake Idamea, near Toko in southwestern Queensland. These modern soils developed on alluvium of the Georgina River, mixed with pisolitic laterite from residual ridges, under mulga (Acacia aneura) shrub steppe (FAO, 1978). Modern climate near Toko is 216 mm mean annual precipitation, 40 mm mean annual range of precipitation, and 31.8 °C mean annual temperature (Bureau of Meteorology, 2018).

Table 2 outlines soil-forming factors inferred for each pedotype. The role of paleotopography, for example, can be inferred from Munsell hue and depth of penetration of root traces. Drab hue is evidence of waterlogging but red hematite is evidence of freely drained paleosols (Lindbo et al., 2010). Roots respire, and will not penetrate anoxic waterlogged ground (Retallack, 1997). Ulye paleosols with gray color, weak granular structure, limited root penetration, and sometimes also tabular carbonate were probably waterlogged soils of permanent waterhole margins or streamsides. The other pedotypes have deeply penetrating roots as well as pedogenic carbonate from soil that dried out at least seasonally (Breecker and Retallack, 2014). Drab-haloed root traces in many of the paleosols are vertical and deeply reaching, but are considered to have formed by burial gleization after subsidence of organic matter below water table for use by anaerobic bacteria (Retallack, 1991b). This mechanism implies that the well-drained paleosols were part of a subsiding floodplain of low relief. One bed of gravel at  $16\,\mathrm{m}$  in the measured section (Fig. 3) shows prominent pebble imbrication. The downstream (uptilted) dip and long orientation of 56 of these pebbles was measured with a Brunton compass to derive a vector mean current flow of 146°, which is orthogonal to the flow direction of modern Waite Creek. This reversal of paleocurrents also affected the Sandover River and may have been due to Pliocene uplift of the MacDonnell Ranges to the south (Senior et al., 1994). Upland landscape reconstructions (Figs. 8-9) are based on connecting currently dissected remnants of the thick laterite underlying the Waite Formation, but retaining modern hills of pre-Miocene rocks.

Parent materials of these paleosols are deeply weathered clays and pisolites redeposited from local laterites, in stark contrast with the shallow calcareous nodules and calcite cements to pisolitic conglomerates (Fig. 3). Content of clay exceeds 50% in all paleosol profiles (Fig. 4), although they appear sandy to conglomeratic in the field. This discrepancy may be due to pisolites and cements (Fig. 5A), and

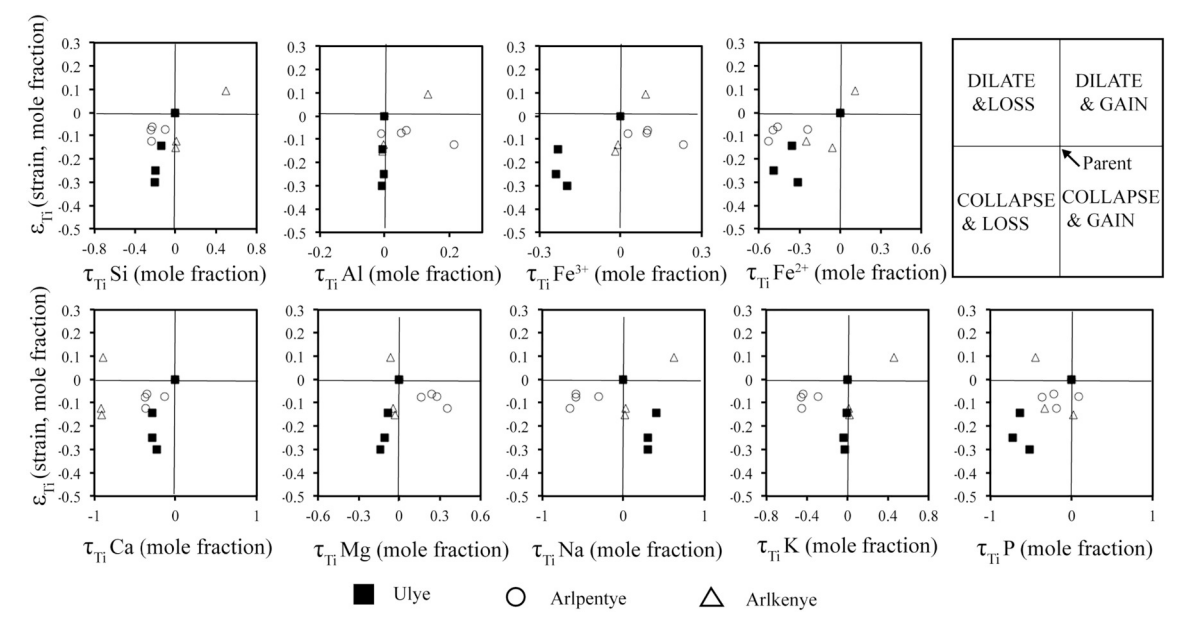


Fig. 6. Mass transport ( $\tau$  mole/mol) and strain ( $\varepsilon$  mole/mol) plotted as deviation from parent materials at origin within non-calcareous matrix of Alcoota paleosols. Strain in soils (y-axis) is usually negative, meaning collapse of volume. Mass transfer (x-axis) in soils is also negative, meaning loss, but can be gain (positive) for redox-sensitive oxides.

scattered sand-sized grains (Fig. 5B) visible in thin section. There is very little silt in these samples, unlike calcareous paleosols of loess (Retallack et al., 2003; Retallack, 2012a). Moderately and weakly developed paleosols are inconsistent with the presence of deeply weathered materials and structures. Red pisolites like those at 7–9 m are usually formed under intense weathering conditions of at least 1100 mm mean annual precipitation and 17 °C mean annual temperature (Retallack, 2010), whereas calcareous soils form under < 800 mm mean annual precipitation (Retallack, 2005). Also, the dominant clay mineral of kaolinite (Fig. 7) represents intense weathering (Retallack, 2010). The deeply weathered sedimentary parent materials derive from erosion of underlying Tertiary laterite nearby (Woodburne, 1967).

Time for formation of calcareous paleosols can be estimated from the diameter of nodules which increase with duration of soil formation (Retallack, 2005). This relationship has been calibrated by radiometric dating of carbonate nodules to derive a relationship between soil age (A in kyrs) and nodule size (S cm; with  $R^2 = 0.57$ , S.E.  $= \pm 1.8$  k.y.), as follows

$$A = 3.92 \cdot S^{0.34} \tag{3}$$

The estimated time duration for calcareous soils is shown in Table 2 and Table 3, whereas the time duration for non-calcareous soils such as Ate and Ulye pedotypes is approximately 100 years or less due to their very weak development. The short time of formation of the Ulye

pedotype is evidence of high rate of deposition (Retallack, 1984) for burial of late Miocene mammals.

#### 7. Vegetation reconstruction

Depth to carbonate in soils is a productivity proxy, reflecting not only mean annual precipitation (Retallack, 2005) and respired soil  $\mathrm{CO}_2$  (Breecker and Retallack, 2014), but the height of trees (Retallack, 2012b). This relationship was different for pteridophytic trees of the Devonian (Retallack and Huang, 2011), and for mesophytic deciduous trees of the northern hemisphere, and the relationship established for evergreen sclerophyll vegetation of Australia was used here (Retallack, 2012b). Most pedotypes in the Waite Formation are Aridisols with calcareous nodules at depth < 30 cm, found under desert shrubland whose height (H, in m) is related to depth (D, in cm) of Bk horizon by the following relationship.

$$H = 12.39 \ln D - 35.74$$
, with  $R^2 = 0.91$ , S. E.  $=\pm 2.3$  m (4)

The reconstructed height of these desert shrublands (Table 3) was generally < 8 m, much lower than typical rainforest (Adam, 1992), and comparable with vegetation around Alcoota today (Carnahan and Deveson, 1990).

Deeply penetrating contorted roots are evidence of woody plants, rather than of grasses or succulents (Retallack, 2001). Paleosol red color

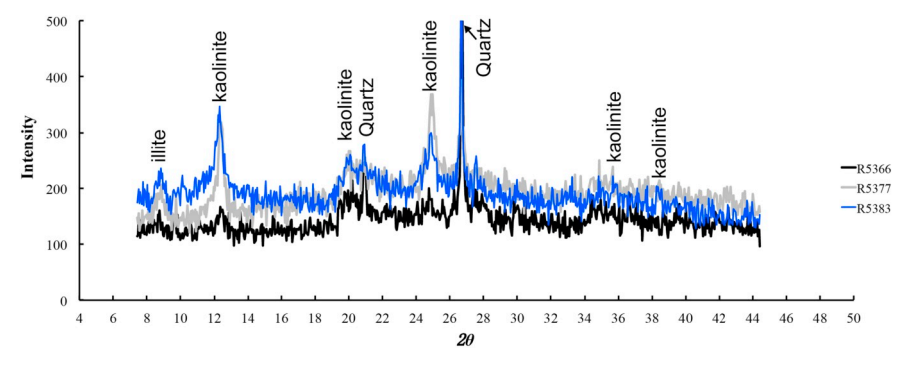


Fig. 7. X-ray diffraction curves of selected samples. Beside quartz, the three samples are dominated by kaolinite with minor illite. R5366 and R5377 are from A horizon of Ulye pedotype. R5383 is from A horizon of Arlpentye pedotype.

 $\begin{tabular}{ll} \bf Table \ 1 \\ \bf Pedotypes \ and \ diagnosis \ for \ Miocene \ paleosols \ at \ Alcoota, \ Northern \ Territory. \end{tabular}$ 

Pedotype (meaning)	Diagenesis	USDA	FAO	Old Australian	New Australian
Ate (lump of dirt) Ahelhe (earth) Arlkenye (multicolored) Arlpentye (tall) Ulye (shade)	te (lump of dirt)  Red sandy surface (A) with small drab-haloed root traces over red surface (Bt) and calcareous nodules (Bk) at < 30 cm  Calcid (Aridisol)  Red sandy surface (A) with drab-haloed root traces over red surface (Bt) at < 30 cm  Calcid (Aridisol)  Red sandy surface (A) with reddish root traces over calcareous nodules (Bk) at < 30 cm  Calcid (Aridisol)  Red sandy surface (A) with reddish root traces over calcareous nodules (Bk) at < 30 cm  Calcid (Aridisol)  Red sandy surface (A) with reddish root traces over calcareous nodules (Bk) at < 30 cm  Calcid (Aridisol)  Red sandy surface (A) with small root traces over gray sandy surface (Bw)	Fluvent (Entisol) Calcid (Aridisol) Calcid (Aridisol) Calcid (Aridisol) Aquept (Inceptisol)	luvent (Entisol) Eutric Fluvisol (Je) Alluvial So calcid (Aridisol) Calcic Xerosol (Xk) Calcareous calcid (Aridisol) Calcic Xerosol (Xk) Calcareous calcid (Aridisol) Calcic Xerosol (Xk) Calcareous vquept (Inceptisol) Haplic Phaeozem (Hh) Gray Clay	Alluvial Soil Calcar Rudosol Calcareous Red Earth Calcic Calcarosol Calcareous Red Earth Calcic Calcarosol Calcareous Red Earth Calcic Calcarosol Gray Clay Gray Clay	Clastic Rudosol Galcic Calcarosol Calcic Calcarosol Calcic Calcarosol Calcic Calcarosol Gray-Orthic Tenosol

Note: Pedotypes were classified by three different systems: USDA (Soil Survey Staff, 2014), FAO (1974, 1978), old Australian (Stace et al., 1968), and new Australian (Isbell, 1996).

 Table 2

 Interpretation of Miocene paleosols at Alcoota, Northern Territory.

Pedotype	Pedotype Paleoclimate	Ecosystem	Parent materials	Palaeotopography	Time for formation (yrs)
Ate	Not diagnostic	Early successional riparian woodland	Quartzofeldspathic sand	Lower riparian levee	Ca. 100
Ahelhe	Arid (250-350), summerwet, warm temperate	Oligotrophic desert shrubland	Pisolitic gravel pediments to laterite scarps	Upper riparian levee	2500-11,600
Arlkenye	Arid (250-350 mm), summerwet, warm temperate	Desert shrubland	Quartzofeldspathic silt	Silty Well drained floodplain	3000-7600
Arlpentye	Arid (250-350 mm), summerwet warm temperate	Desert shrubland	Quartzofeldspathic conglomerate and sand	Well drained floodplain	0008-0089
Ulye	Not diagnostic	Waterhole gallery woodland	Quartzofeldspathic silt and kaolintic claystone	Poorly drained waterhole margin	Ca. 100

Note: Paleoprecipitation of calcareous pedotypes (Ahelhe, Arlhentye, Arlpentye) was estimated by depth (cm) to Bk. Time for formation is based on calcareous nodule diameter (cm). See Table 3 for details. Pedotypes (Ate and Ulye) with no Bk horizon are not diagnostic of paleoclimate.

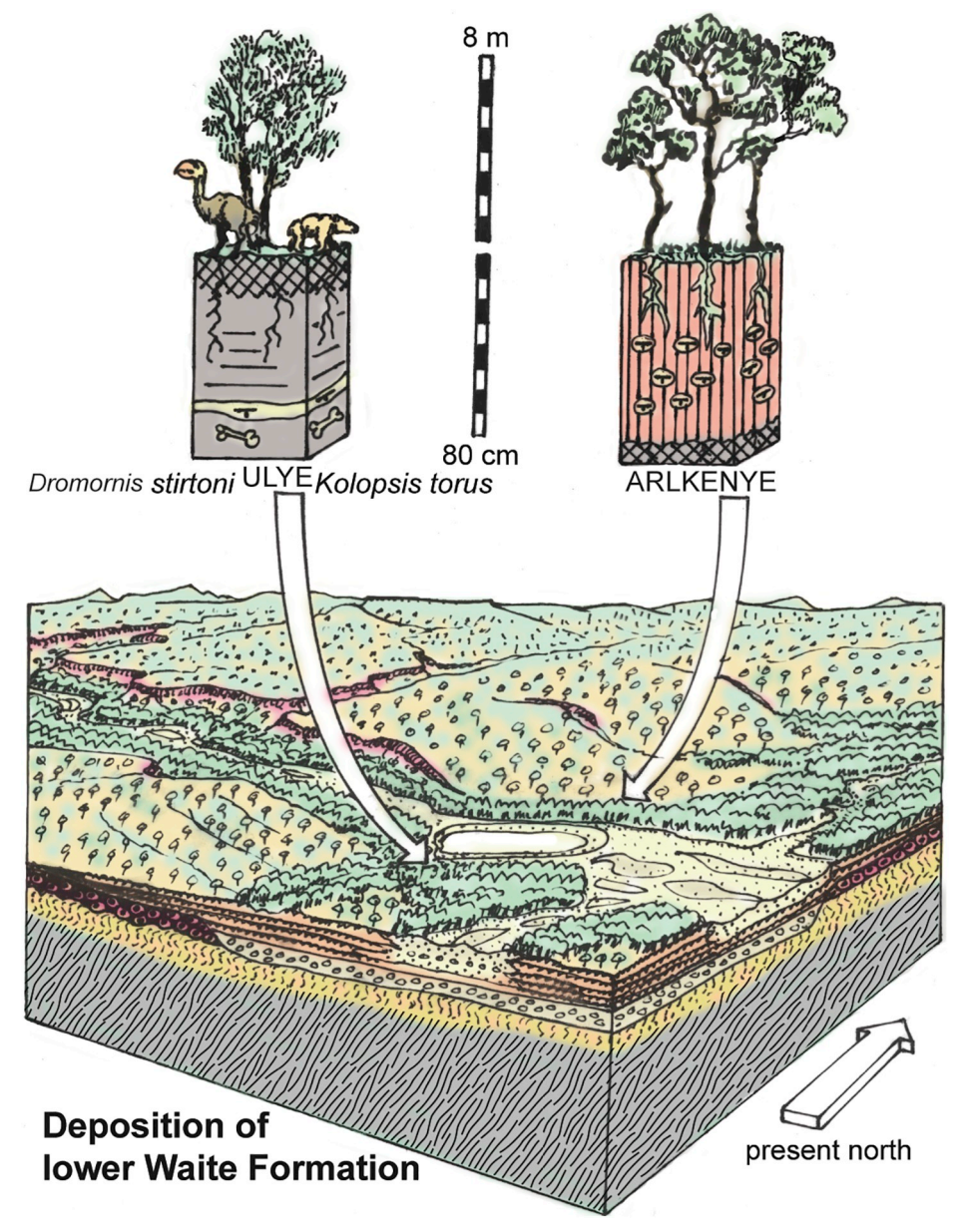


Fig. 8. Reconstruction of Alcoota local fauna level of Waite Formation (ca. 10 Ma).

and sandy to gravelly texture is evidence of vegetation of well drained floodplains and riparian zones (Lindbo et al., 2010). Two exceptions are the gray and weakly developed Ulye pedotype, with sparse and shallow root traces above bone bearing sands and gravels. These paleosols contain both the Alcoota and Ongeva local faunas, considered to have accumulated in droughts because of waterhole tethering of animals (Murray and Vickers-Rich, 2004). Common trees in waterlogged depressions of Northern Territory today with soils like Ulye pedotype (Fig. 8) are paperbarks (Melaleuca leucadendra and M. argentea; O'Grady et al., 2006). Common trees of outback Australian gravelly river margins like Arlpentye pedotype (Fig. 9) today are river red gum (Eucalyptus camaldulensis: Gibson et al., 1994) and ghost gum (Corymbia bella: O'Grady et al., 2006) (Fig. 9). Common on lateritic residual soils such as Ahelhe pedotype (Fig. 9) is mulga (Acacia aneura: Dawson and Ahern, 1973; Miller et al., 2002; Bowman et al., 2008).

The Miocene faunas of Alcoota and Ongeva local faunas include kangaroos, but no grazers (Murray and Vickers-Rich, 2004; Retallack, 2012b), so grasses were probably uncommon. In contrast with desert vegetation and soils similar to modern from some 5–12 Ma at Alcoota

are laterites underling the Waite Formation, probably 12-16 Ma in age, like other laterites of Northern Territory (Dammer et al., 1996). Such deeply weathered profiles are produced by wet ( $> 1100\,\mathrm{mm}$  mean annual precipitation) tropical (> 17 °C mean annual temperature) paleoclimates under rainforest. A modern analog for such forests may be closed monsoon vine forests of Holmes Jungle, Northern Territory (Murray and Vickers-Rich, 2004). Rain forests more like those creating lateritic profiles elsewhere in the world (Retallack, 2010) are better known in northeast Que.ensland (Carnahan and Deveson, 1990). Thus under high CO2, and warmer and wetter paleoclimate of the middle Miocene rainforests may have migrated as far south as Alcoota. Such Neogene migrations have been thought to explain relict cabbage palms (Livistona mariae) in Palm Valley, western Macdonnell Ranges (latitude 24°S), Northern Territory (Wischusen et al., 2004). However, these particular palms may have been planted between 7 and 31 ka by aboriginals from the Roper River at 14°S or Gregory River at 18°S to the north and east, as revealed by DNA similarities (Kondo et al., 2012) and aboriginal legend (Bowman et al., 2015). Nevertheless the wider distribution of tropical cabbage palms (Livistona australis) as far south as

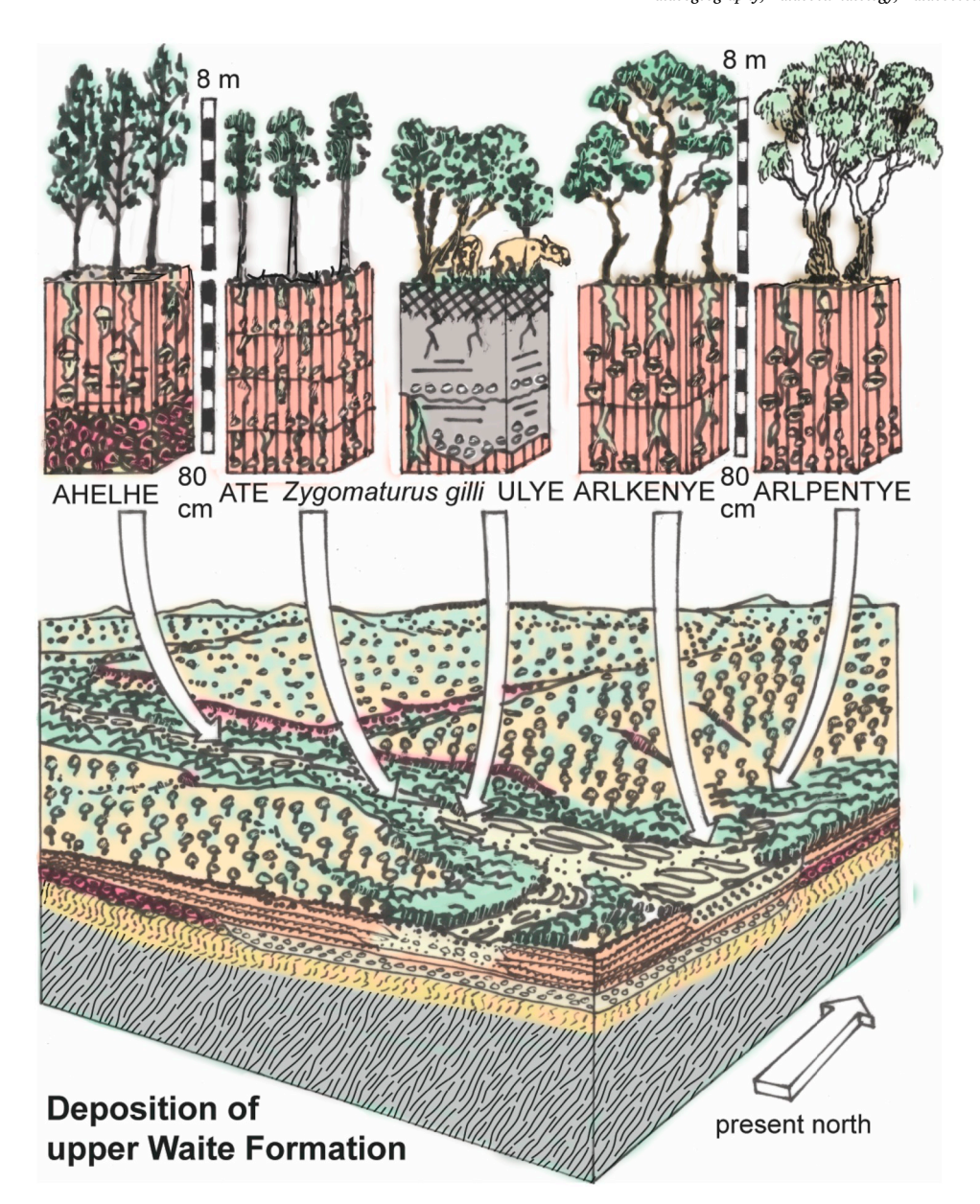


Fig. 9. Reconstruction of Ongeva local fauna level of Waite Formation (ca. 8 Ma).

**Table 3**Paleoclimate, soil duration and tree height for Miocene paleosols of Alcoota, Northern Territory.

Pedotype	Depth (m)	Age (Ka)	Depth to Bk (cm)	Bk thickness (cm)	Nodule size (cm)	MAP ( ± 147 mm)	MARP ( ± 22 mm)	Time of formation ( $\pm 1.8 \mathrm{ka}$ )	Tree height ( $\pm 2.3 \mathrm{m}$ )
Arlpentye	18.8	5.9	27	22	4	302	31.1	6.3	5.1
Arlpentye	18.2	6.1	25	22	3	290	31.1	5.7	4.1
Arlpentye	17.2	6.3	28	21	2	308	30.3	5.0	5.5
Arlpentye	15.7	6.6	23	16	3	279	26.3	5.7	3.1
Arlpentye	13.9	7.0	27	25	2	302	33.5	5.0	5.1
Ahelhe	12.5	7.3	32	16	1.3	330	26.3	4.3	7.2
Arlkenye	12	7.4	26	18	3.2	296	27.9	5.8	4.6
Arlkenye	11.4	7.6	23	14	2.5	279	24.8	5.4	3.1
Arlkenye	10.8	7.7	21	13	1.8	267	24.0	4.8	2.0
Ahelhe	9.3	8.0	24	21	3	285	30.3	5.7	3.6
Ahelhe	7.7	8.4	29	24	5	313	32.7	6.8	6.0
Ahelhe	7.2	8.5	20	21	15	261	30.3	9.8	1.4
Ahelhe	6.6	8.6	19	13	4	255	24.0	6.3	0.7
Ahelhe	6.3	8.7	21	16	3	267	26.3	5.7	2.0
Arlkenye	1.8	9.7	25	16	3	290	26.3	5.7	4.1

Note: Paleoclimate reconstruction based on depth to Bk, Bk thickness, and calcareous nodule size (Retallack, 2005). Tree height is reconstructed based on depth to Bk horizon (Retallack, 2012b).

Bermagui in NSW (37°S), and (*L. nasmophila*) in Purnululu, Western Australia (17°S) may be relict from the middle Miocene, judging from molecular dating of choroplast and nuclear DNA (Crisp et al., 2010). Lateritic profiles of middle Miocene age as far south as Sydney, New South Wales (34°S) support the idea of rain forest climate far to the south at that time (Retallack, 2010). Other relict rainforest taxa persisting in fire-protected patches of Northern Territory aridlands are bullwaddie (*Macropteranthes*), rosary pea (*Abrus*), sarsaparilla tree (*Alphitonia*), phalsa (*Grewia*), stinkwood (*Gyrocarpus*), and strychnine tree (*Strychnos*: Adam, 1999). These rainforest relicts have large fruits proposed as essential dietary items for the giant birds, *Dromornis stirtoni* of the Alcoota local fauna, and cf. *Dromornis* and cf. *Ilbandornis* of the Ongeva local fauna (Murray and Vickers-Rich, 2004).

Wet rainforests did not extend much south of the MacDonnell Ranges, because the middle Miocene greenhouse spike near Lake Palankarinna, South Australia (29°S) supported mallee vegetation, not rain forest (Metzger and Retallack, 2010). Rainforests of the Miocene were diverse like those of tropical Australia today (Archer et al., 1994; Travouillon et al., 2009), and their retreat into refugia since the late Miocene may be partly reversed with global climate change in the next century (Retallack et al., 2016).

### 8. Paleoclimate reconstruction

A perennial debate is when the aridity started in the Australian outback and over how much of the continent (Archer et al., 1995; Herold et al., 2011). Fossil floras and faunas reflect general paleoclimate and paleovegetation (Archer et al., 1995), but evidence from paleosols is also useful (Metzger and Retallack, 2010), and increasingly well quantified (Sheldon and Tabor, 2009). Calcareous paleosols in our section near Alcoota reveal the onset of Miocene aridity (Retallack, 2005).

Geochemical climofunctions (Sheldon and Tabor, 2009) based on chemical ratios of B horizons within individual soil profiles have been proposed as proxies for mean annual precipitation (*MAP*) following Eq. (5) (Sheldon et al., 2002).

$$MAP = 221.1e^{0.0197(CIA-K)}$$
, with  $R^2 = 0.72$ , S. E.  $=\pm 182$  mm. (5)

where CIA-K is the molar ratio of  $100 \times Al_2O_3/(Al_2O_3 + CaO + Na_2O)$ . However, the attempt to reconstruct Alcoota MAP in this way yielded unrealistic values:  $> 1200\,\mathrm{mm}$ , because these paleosols developed on redeposited, deeply weathered pisolitic laterite with only local carbonate nodules. This and other chemically based methods are thus discarded.

Pedogenic calcareous nodules (Bk horizon) in soil profiles are better proxies for amount and seasonality of precipitation (Retallack, 2005). Mean annual precipitation (MAP) and mean annual range of precipitation (MARP, the difference between monthly means of wettest and driest months) can be quantitatively reconstructed based on the depth (cm) to Bk horizon and the thickness (cm) of Bk horizon, respectively, following Eqs. (6) and (7).

$$MAP \text{ (mm)} = -0.013D^2 + 6.45D + 137.2$$
, with  $R^2 = 0.52$ , S. E.  $=\pm 147 \text{ mm/y}$ .

(6)

where D is depth (cm) to Bk.

$$MARP$$
 (mm) = 0.79 $T$  + 13.7, with  $R^2$  = 0.58, S. E. =±22 mm/y. (7)

where T is thickness of Bk.

Reconstructed MAP for the late Miocene in central Australia ranges from 100 mm to 400 mm with MARP up to 50 mm (Fig. 10A). This paleoclimate is similar to modern Alcoota with MAP 296 mm and MARP 56 mm, and to modern Alice Springs with MAP 282 mm and MARP 33 mm (Bureau of Meteorology, 2018). It is thus neither a rainforest (> 1100 mm MAP) nor monsoonal (> 100 mm MARP) climate. Ephemeral pools or rivers existed for a short period to accumulate lacustrine and fluvial sediments around Alcoota (Fig. 3). This result is

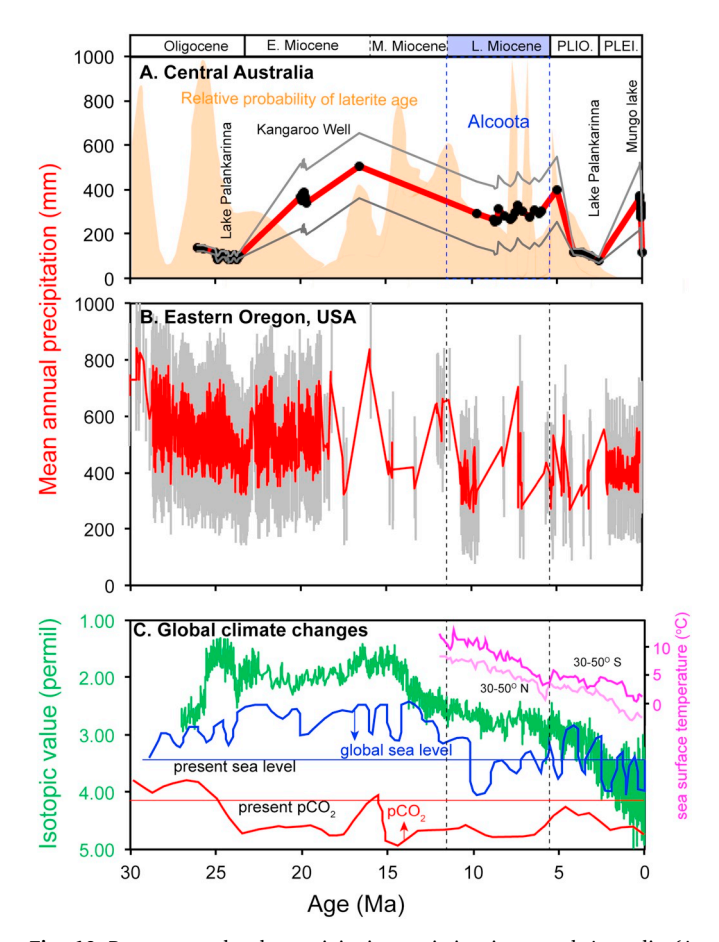


Fig. 10. Reconstructed paleoprecipitation variation in central Australia (A, from Metzger and Retallack, 2010) and comparison to that in eastern Oregon, USA (B, from Retallack, 2007) based on depth to Bk horizons in paleosol profiles. The gray curve or bars in (A) and (B) represent error range. (C) Global climate changes from late Oligocene to present; oxygen isotope variation from late Oligocene to present (Zachos et al., 2001), global sea level variation from late Oligocene to present (Haq et al., 1987), global atmospheric  $CO_2$  from late Oligocene to present (Beerling and Royer, 2011), sea surface temperature from late Miocene to present (Herbert et al., 2016). Laterite age probability (A) is from Dammer et al. (1996).

similar to early Miocene arid climate (200-600 mm MAP, up to 50 mm MARP) in near Kangaroo Well (Dammer et al., 1996; Metzger and Retallack, 2010) (Fig. 10A), 150 km south of Alcoota. Thus arid climate in central Australia started in the early Miocene (Murray and Megirian, 1992), was interrupted by middle Miocene warm-wet spikes (Metzger and Retallack, 2010), and resumed in the late Miocene. Continental drying likely developed from the south, because arid Oligocene paleoclimate (< 200 mm MAP) was inferred around Lake Palankarina in South Australia from paleosols with gypsum nodules (Metzger and Retallack, 2010) (Fig. 10A). If aridity spread from the south, the warmwet climate spike spread tropical northern rainforests southward forming lateritic and bauxitic paleosols. The abundance of arboreal mammals and high species diversity near Riversleigh in northwest Queesnland are evidence of wet rainforest climate during the middle Miocene (Archer et al., 1995), when laterites expanded to Alcoota. Fossil plants however are evidence for dry climates in northern Australia before and after this middle Miocene warm-wet spike (Hill, 1994; Guerin and Hill, 2006; Hill et al., 2016). After the middle Miocene, rainforest retracted to northern Australia. Central Australia thus became arid in the early Miocene, then humid in the middle Miocene, and arid again by late Miocene.

Late Miocene drying was a global phenomenon (Fig. 10). Late Miocene drying in central Australia coincides with global cooling

inferred from isotopic studies of deep-sea cores worldwide (Zachos et al., 2001: Herbert et al., 2016). Central Australian aridity in the early and late, but not middle Miocene is comparable with paleosol records in Oregon (Retallack, 2007), northwest USA (Fig. 10B). Oligocene cooling and drying coincided with appearance of Antarctic ice-sheet and late Miocene cooling with advances of northern hemisphere ice (Zachos et al., 2001). Haq et al. (1987) show that global sea level decreased more during the late Miocene than early and middle Miocene (Fig. 10C). Herbert et al. (2016) attribute global cooling in late Miocene to decreased atmospheric CO<sub>2</sub> (Beerling and Royer, 2011). The decline in atmospheric CO<sub>2</sub> has in turn been attributed to Himalayan uplift (Raymo and Ruddiman, 1992), southern ocean reorganization (Kennett, 1977), or expansion of grassland soils (Retallack, 2013).

#### 9. Conclusions

The antiquity of Miocene aridity in central Australia was addressed by studying late Miocene paleosols near Alcoota, Northern Territory. In a 19-m-thick stratigraphic section including stratigraphic levels with Ongeva and Alcoota local faunas, 19 paleosols of 5 different pedotypes were investigated in detail. Most paleosols included shallow Bk horizon of pedogenic calcareous nodules, developed on redeposited middle Miocene lateritic pisolites and clays. Unlike the lateritic paleosols formed under rainforests of the middle Miocene, the depth to Bk horizon and Bk thickness of late Miocene paleosols are evidence of mean annual precipitation ranging from 100 mm to 400 mm and mean annual range of precipitation up to 50 mm. This arid climate is similar to that of modern central Australia, thus neither a rainforest nor monsoonal paleoclimate. Paleovegetation of open woodland and gallery woodland < 8 m was inferred from depth to carbonate, root traces and modern analogs of the paleosols. Late Miocene drying in central Australia coincides with global cooling and drying with declining atmospheric CO<sub>2</sub>, but future warmer and wetter climate with rising CO<sub>2</sub> may bring rainforest vegetation southward again.

## Acknowledgments

This work is financially supported by National Natural Science Foundation of China (Grant No. 41602184, 41772180), Scientific grants of Fujian province (Grant No. 2015R1034-5, 2017J01655, U1405281), creative group grant from Fujian Normal University (IRTL1705), and scholarship from Education department of Fujian Province. Field advice and permissions were facilitated by Peter Murray and Dirk Megirian of the Museum and Art Gallery of Northern Territory, Alice Springs.

## Appendix A. Supplementary data

Supplementary data to this article can be found online at https://doi.org/10.1016/j.palaeo.2018.10.008.

#### References

- Adam, P., 1992. Australian Rainforests. Oxford University Press, Oxford.
- Archer, M., Hand, S.J., Godthelp, H., 1994. Riversleigh: The Story of Animals in Ancient Rainforests of Inland Australia. Reed, Sydney.
- Archer, M., Haven, N., Hand, S.J., Godthelp, H., 1995. Environmental and biotic change in the Tertiary of Australia. In: Vrba, E., Denton, G., Partridge, T. (Eds.), Paleoclimate and Evolution, With Emphasis on Human Origins. Yale University Press, New Haven, pp. 77–90.
- Beerling, D.J., Royer, D.L., 2011. Convergent Cenozoic CO<sub>2</sub> history. Nat. Geosci. 4, 418–420.
- Bowman, D.M.J.S., Boggs, G.S., Prior, L.D., 2008. Fire maintains an Acacia aneura shrubland—*Triodia* grassland mosaic in central Australia. J. Arid Environ. 72, 34–47. Bowman, D.M.J.S., Gibson, J., Kondo, T., 2015. Outback palms: Aboriginal myth meets DNA analysis. Nature 520, 33.
- Breecker, D.O., Retallack, G.J., 2014. Refining the pedogenic carbonate atmospheric CO<sub>2</sub> proxy and application to Miocene CO<sub>2</sub>. Palaeogeogr. Palaeoclimatol. Palaeoecol. 406, 1–8.

- Breecker, D.O., Sharp, Z.D., McFadden, L.D., 2010. Atmospheric CO<sub>2</sub> concentrations during ancient greenhouse climates were similar to those predicted for AD 2100. Proc. Natl. Acad. Sci. 107, 576–580.
- Brimhall, G.H., Chadwick, O.A., Lewis, C.J., Compston, W., Williams, I.S., Danti, K.J., Dietrich, W.E., Power, M.E., Hendricks, D., Bratt, J., 1992. Deformational mass transport and invasive processes in soil evolution. Science 255, 695–702.
- Bureau of Meteorology, Australia, 2018. Alcoota. Website. http://www.bom.gov.au/, Accessed date: 16 July 2018.
- Carnahan, J., Deveson, T., 1990. Atlas of Australian Resources, v.6. Vegetation. Australian Surveying and Land Information Group, Canberra
- Crisp, M.D., Isagi, Y., Kato, Y., Cook, L.G., Bowman, D.M., 2010. Livistona palms in Australia: ancient relics or opportunistic immigrants? Mol. Phylogenet. Evol. 54, 512–523
- Dammer, D., Chivas, A.R., McDougall, I., 1996. Isotopic dating of supergene manganese oxides from the Groote Eylandt deposit, Northern Territory, Australia. Econ. Geol. 91, 386–401
- Dawson, N.M., Ahern, C.R., 1973. Soils and landscapes of mulga lands with special reference to south western Queensland. Trop. Grasslands 7, 23–34.
- FAO, 1974. Soil Map of the World, v. 1 Legend. UNESCO, Paris.
- FAO, 1978. Soil map of the world, v. X. Australasia. UNESCO, Paris.
- Gibson, A., Bachelard, E.P., Hubick, K.T., 1994. Growth strategies of *Eucalyptus ca-maldulensis* Dehnh. at three sites in northern Australia. Funct. Plant Biol. 21, 653–662.
- Green, J., 1994. A learner's guide to Eastern and Central Arrernte. IAD Press, Alice Spring. Guerin, G.R., Hill, R.S., 2006. Plant macrofossil evidence for the environment associated with the Riversleigh fauna. Aust. J. Bot. 54, 717–731.
- Haq, B.U., Hardenbol, J., Vail, P., 1987. Chronology of fluctuating sea levels since the Triassic. Science 235, 1156–1167.
- Henderson, J., Dobson, V., 1994. Eastern and Central Arrernte to English Dictionary. IAD Press, Alice Spring.
- Herbert, T.D., Lawrence, K.T., Tzanova, A., Peterson, L.C., Caballero-Gill, R., Kelly, C.S., 2016. Late Miocene global cooling and the rise of modern ecosystems. Nat. Geosci. 9, 843–847.
- Herold, N., Huber, M., Greenwood, D.R., Müllerm, R.D., Seton, M., 2011. Early to middle Miocene monsoon climate in Australia. Geology 39, 3–6.
- Hill, R.S., 1994. History of the Australian Vegetation: Cretaceous to Recent. University of Adelaide Press.
- Hill, R.S., Beer, Y.K., Hill, K.E., Maciunas, E., Tarran, M.A., Wainman, C.C., 2016. Evolution of the eucalypts—an interpretation from the macrofossil record. Aust. J. Bot. 64, 600–608.
- Isbell, R.F., 1996. The Australian Soil Classification. CSIRO Publishing Melbourne. Kennett, J.P., 1977. Cenozoic evolution of Antarctic glaciation: the circum-Antarctic oceans and their impact on global paleoceanography. J. Geophys. Res. 82, 3843–3859.
- Kondo, T., Crisp, M.D., Linde, C., Bowman, D.M., Kawamura, K., Kaneko, S., Isagi, Y., 2012. Not an ancient relic: the endemic *Livistona* palms of arid central Australia could have been introduced by humans. R. Soc. London Proc. B279, 2652–2661.
- Lindbo, D.L., Stolt, M.H., Vepraskas, M.J., 2010. Redoximorphic features. In: Stoops, G., Marcelino, V., Mees, F. (Eds.), Interpretation of Micromorphological Features of Soils and Regoliths. Elsevier, Amsterdam, pp. 129–147.
- Megirian, D., Murray, P., Wells, R., 1996. The late Miocene Ongeva local fauna of central Australia. In: The Beagle: Records of the Museums and Art Galleries of the Northern Territory. 13. pp. 9–38.
- Megirian, D., Murray, P., Schwartz, L.R.S., von der Borch, C., 2004. Late Oligocene Kangaroo well local fauna from the Ulta Limestone (new name) and climate of the Miocene oscillation across central Australia. Aust. J. Earth Sci. 51, 701–741.
- Megirian, D., Prideaux, G.J., Murray, P.F., Smit, N., 2010. An Australian land mammal age biochronological scheme. Paleobiology 36, 658–671.
- Metzger, C.A., Retallack, G.J., 2010. Paleosol record of Neogene climate change in the Australian outback. Aust. J. Earth Sci. 57, 871–885.
- Miller, J.T., Andrew, R.A., Maslin, B.R., 2002. Towards an understanding of variation in the Mulga complex (*Acacia aneura* and relatives). Conserv. Sci. West. Aust. 4, 19–35.
- Murray, P., Megirian, D., 1992. Continuity and contrast in middle and late Miocene vertebrate communities from the Northern Territory. In: The Beagle: Records of the Museums and Art Galleries of the Northern Territory. vol. 9. pp. 195–218.
- Murray, P.F., Vickers-Rich, P., 2004. Magnificent Mihirungs: The Colossal Flightless Birds of the Australian Dreamtime. Indiana University Press.
- Novoselov, A.A., de Souza Filho, C.R., 2015. Potassium metasomatism of Precambrian paleosols. Precambrian Res. 262, 67–83.
- O'Grady, A.P., Eamus, D., Cook, P.G., Lamontagne, S., 2006. Groundwater use by riparian vegetation in the wet-dry tropics of northern Australia. Aust. J. Bot. 54, 145–154.
- Raymo, M.E., Ruddiman, W.F., 1992. Tectonic forcing of late Cenozoic climate. Nature 359, 117–122.
- Retallack, G., 1984. Completeness of the rock and fossil record: some estimates using fossil soils. Paleobiology 10, 59–78.
- Retallack, G., 1991a. Miocene Paleosols and Ape Habitats in Pakistan and Kenya. Oxford University Press, New York.
- Retallack, G.J., 1991b. Untangling the effects of burial alteration and ancient soil formation. Annu. Rev. Earth Planet. Sci. 19, 183–206.
- Retallack, G.J., 1997. A Colour Guide to Paleosols. John Wiley and Sons, Chichester.Retallack, G.J., 2001. Soils of the Past: An Introduction to Paleopedology. Blackwell Science Ltd, Oxford, UK.
- Retallack, G.J., 2005. Pedogenic carbonate proxies for amount and seasonality of precipitation in paleosols. Geology 33, 333–336.
- Retallack, G.J., 2007. Cenozoic paleoclimate on land in North America. J. Geol. 115, 271–294.

- Retallack, G.J., 2010. Lateritization and bauxitization events. Econ. Geol. 105, 655–667.Retallack, G.J., 2012a. Were Ediacaran siliciclastics of South Australia coastal or deep marine? Sedimentology 59, 1208–1236.
- Retallack, G.J., 2012b. Mallee model for Mesozoic and early Cenozoic mammalian communities. Palaeogeogr. Palaeoclimatol. Palaeoecol. 342–343, 111–129.
- Retallack, G.J., 2013. Global cooling by grasslands in the geological past and near future. Annu. Rev. Earth Planet. Sci. 41, 5.1–18.
- Retallack, G.J., Huang, C.-M., 2011. Ecology and evolution of Devonian trees in New York, USA. Palaeogeogr. Palaeoclimatol. Palaeoecol. 299, 110–128.
- Retallack, G.J., Smith, R.M.H., Ward, P.D., 2003. Vertebrate extinction across the Permian-Triassic boundary in the Karoo Basin of South Africa. Bull. Geol. Soc. Am. 115. 1133–1152.
- Retallack, G.J., Gavin, D.G., Davis, E.B., Sheldon, N.D., Erlandson, J.M., Reed, M.H., Bestland, E.A., Roering, J.J., Carson, R.J., Mitchell, R.B., 2016. Oregon 2100: projected climatic and ecological changes. In: University of Oregon Museum of Natural and Cultural History Bulletin. 26. pp. 1–21.
- Retallack, G.J., Bajpai, S., Liu, X., Kapur, V.V., Pandey, S.K., 2018a. Advent of strong Indian monsoon by 20 million years ago. J. Geol. 126, 1–24.
- Retallack, G.J., Broz, A., Breithaupt, B., Matthews, N., Martin, J.E., 2018b. Pleistocene mammoth trackway from Fossil Lake, Oregon. Palaeogeogr. Palaeoclimatol. Palaeoecol. 496, 192–204.
- Rohde, C., 2005. Alcoota Project EL9803 Final Report. Tanami Exploration N.L, Subisaco, Western Australia.
- Senior, B.R., Truswell, E.M., Idnurm, M., Shaw, R.D., Warren, R.G., 1994. Cainozoic sedimentary basins in the eastern Arunta Block, Alice Springs region, central Australia.

- AGSO J. Aust. Geol. Geophys. 15, 421-444.
- Shaw, R.D. and Warren, R.G. 1975. Alcoota, First Edition 1:250,000 scale geological map and notes. Bureau of Mineral Resources, Geology and Geophysics, Canberra.
- Sheldon, N.D., Retallack, G.J., 2001. Equation for compaction of paleosols due to burial. Geology 29, 247–250.
- Sheldon, N.D., Tabor, N.J., 2009. Quantitative paleoenvironmental and paleoclimatic reconstruction using paleosols. Earth Sci. Rev. 95, 1–52.
- Sheldon, N.D., Retallack, G.J., Tanaka, S., 2002. Geochemical climofunctions from North American soils and application to paleosols across the Eocene-Oligocene boundary in Oregon. J. Geol. 110, 687–696.
- Soil Survey Staff, 2014. Key to Soil Taxonomy. Pocahontas Press, Blacksburg, Virginia. Stace, H.C.T., Hubble, G.D., Brewer, R., Northcote, K.H., Sleeman, J.R., Mulcahy, M.J., Hallsworth, E.G., 1968. A Handbook of Australian Soils. Rellim, Adelaide.
- Tate, T., Retallack, G., 1995. Thin sections of paleosols. J. Sediment. Res. A65, 579–580.
   Travouillon, K.J., Legendre, S., Archer, M., Hand, S.J., 2009. Palaeoecological analyses of Riversleigh's Oligo-Miocene sites: implications for Oligo-Miocene climate change in Australia. Palaeogeogr. Palaeoclimatol. Palaeoecol. 276, 24–37.
- Wischusen, J.D., Fifield, L.K., Cresswell, R.G., 2004. Hydrogeology of Palm Valley, central Australia; a Pleistocene flora refuge? J. Hydrol. 293, 20–46.
- Woodburne, M.O., 1967. The Alcoota fauna, central Australia: an integrated paleontological and geological study. Bur. Mineral. Resour. Geol. Geophys. Aust. Bull. 87, 1–187
- Zachos, J., Pagani, M., Sloan, L., Thomas, E., Billups, K., 2001. Trends, rhythms, and aberrations in global climate 65 Ma to present. Science 292, 686–693.